Volume 58
Number 92
28 November 2022
Pages 12743–12888

ChemComm

Chemical Communications

rsc.li/chemcomm

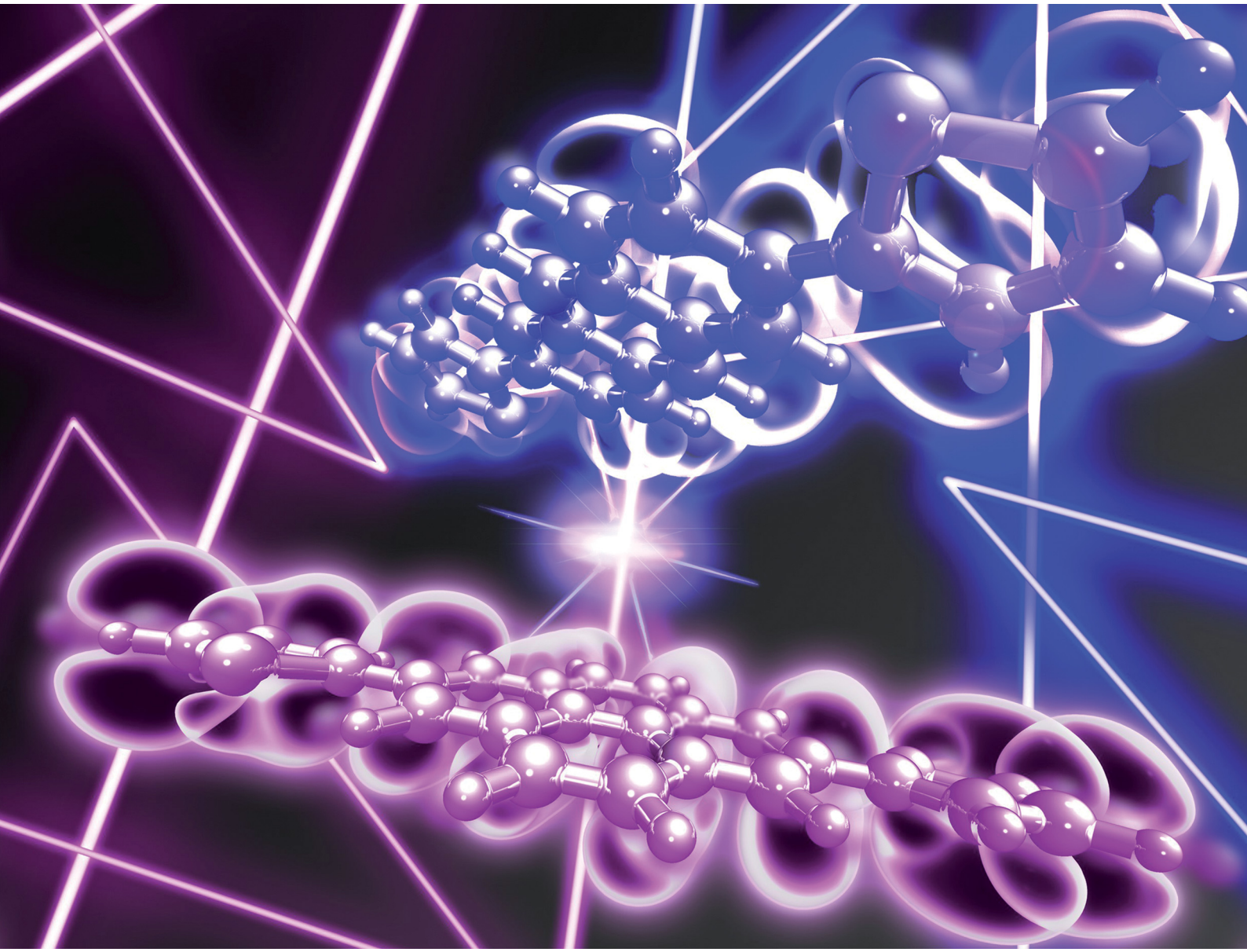

ISSN 1359-7345

ROYAL SOCIETY OF CHEMISTRY

COMMUNICATION

Michael T. Ruggiero *et al.*

Side-chain torsional dynamics strongly influence charge transport in organic semiconductors

ChemComm

ROYAL SOCIETY OF CHEMISTRY

COMMUNICATION

View Article Online
View Journal | View Issue

Cite this: *Chem. Commun.*, 2022, **58**, 12803

Received 8th September 2022,
Accepted 12th October 2022

DOI: 10.1039/d2cc04979a

rsc.li/chemcomm

Side-chain torsional dynamics strongly influence charge transport in organic semiconductors†

Peter A. Banks, Adam M. Dyer, Adam C. Whalley and Michael T. Ruggiero *

The role of low-frequency (terahertz) vibrational motions on charge carrier dynamics in organic semiconductors (OSCs) is becoming well-known, and efforts are underway to rationally design new materials to mitigate these detrimental effects. However, most efforts have focused on stabilizing the fused-ring semiconducting 'core', often by functionalizing with various side-groups, yet questions regarding the role of such modifications on electron–phonon couplings are still outstanding. In this work, the influence of thiophene rings σ-bonded directly to the π-conjugated cores is explored. The manner in which these groups alter low-frequency vibrational, and resulting electronic, dynamics is quantified using a theoretical approach employing fully-periodic density functional theory (DFT) simulations. Ultimately, these results showcase how the equilibrium geometry and corresponding electronic structure are directly related to detrimental electron–phonon coupling, which have important implications for the design of improved organic optoelectronic materials.

OSCs have been the subject of immense study over the past several decades owing to their unique molecular nature, which affords numerous benefits such as low-cost bench-top solution processing and fascinating electronic properties due to their extended π-conjugation.[1] Because OSCs often crystallize through weak non-covalent interactions, such as van der Waals forces and π-stacking, additional factors arise that both promote – and inhibit – charge transport. Specifically, the weak intermolecular forces that exist in these materials give rise to large-amplitude low-frequency (terahertz) vibrations that severely limit carrier mobilities through electron–phonon coupling – a phenomenon commonly referred to as "dynamic disorder."[2–4] Recently, there have been reports involving the "rational" design of molecules specifically purposed to suppress detrimental low-frequency molecular motions, while simultaneously attempting to improve the electronic structure, ultimately in search of molecular properties that drive the design of next generation OSCs.[5,6] However, no such broad guiding principles currently exist. Side-group functionalization, such as alkylation, has been of particular interest, owing to both the previously reported effects on low-frequency dynamics and device performance, as well as the synthetically diverse scope of coupling reactions that are commonly used to install these linkages.[5,7,8] Additionally, collective motion of sterically-bulky alkyl side-chains has been attributed to martensitic phase transformations in these materials, enabling the prospect of shape memory devices, as well as accessing previously unobtainable crystalline polymorphs.[9]

In an attempt to install more electronically-relevant side-groups, a number of molecules have been synthesized with σ-bonded thiophene rings, which were specifically introduced to enhance intermolecular π–π and S–π interactions to further reinforce charge transport in these materials.[10–13] However, the specific influence of installing such groups on the low-frequency dynamics, and associated electron–phonon couplings that plague these materials, remains largely unknown. In order to investigate the impact of σ-bonded thiophene groups on both intermolecular electronic couplings and low-frequency vibrational dynamics, four organic semiconducting molecular crystals bearing similar σ-bonded thiophene subtituents were initially selected as model systems, including: 2,7-bis(thiophen-2-yl)-pyrene (DT-P),[11] 2,6-(thien-2-yl)anthracene (DT-Ant),[12] 6,13-bis(5-hexylthiophene-2-yl)pentacene (DT-Pen),[13] and a newly-synthesized benzothienobenzothiophene (BTBT) derivative, 3,8-bis(5-hexylthiophen-2-yl)benzo[*b*]benzo-[4,5]thieno[2,3-*d*]thiophene (C6-DT-BTBT), which are shown in Fig. 1.

C6-DT-BTBT was synthesized using a Suzuki–Miyaura coupling of a 3,8-triflate-BTBT precursor and an alkylated thiophene boronic ester, yielding the desired product.[14] Single crystals were obtained from recrystallization from $CHCl_3$ and MeOH, affording yellow needles suitable for single-crystal X-ray

Department of Chemistry, University of Vermont, 82 University Place, Burlington, Vermont 05405, USA. E-mail: michael.ruggiero@uvm.edu

† Electronic supplementary information (ESI) available: Synthetic methods of C6-DT-BTBT, diffraction experiment details, theoretical methods of periodic and dimer projection simulations, and full analyses of electron-phonon couplings for the investigated materials. CCDC 2206129. For ESI and crystallographic data in CIF or other electronic format see DOI: https://doi.org/10.1039/d2cc04979a

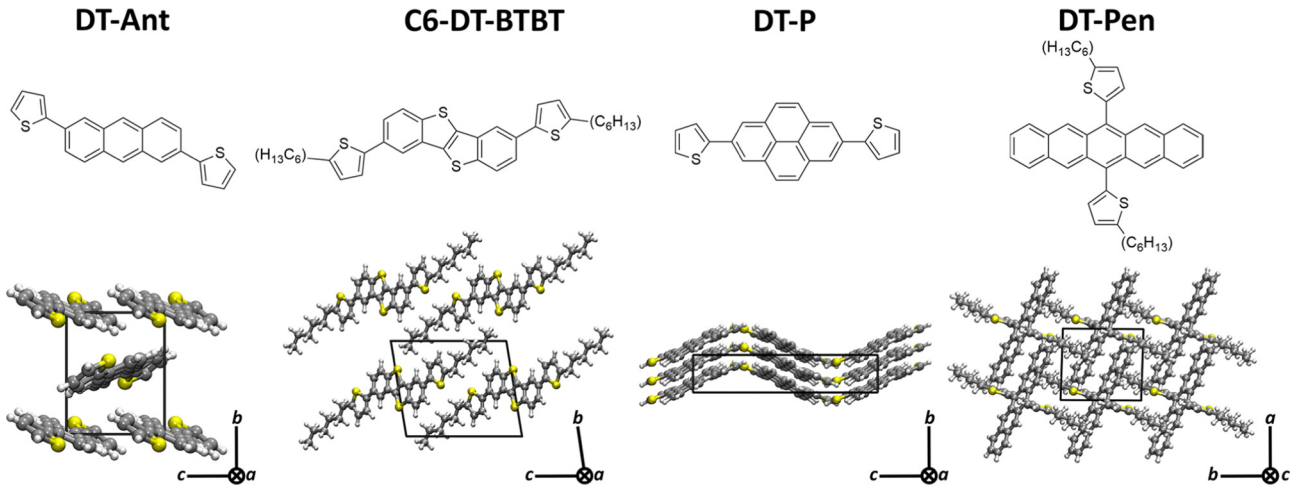

Fig. 1 Molecular structures (top) and crystalline packing (bottom) of the investigated materials.

diffraction. All other crystalline structures were obtained from the reported single-crystal X-ray diffraction experiments.[11–13] Additional synthetic and experimental details are available in the ESI.†

Using the structures obtained with single-crystal X-ray diffraction experiments, each solid was modeled using fully-periodic DFT simulations with the Crystal17 package, using the GGA PBE density functional with Grimme's dispersion corrections and Becke–Johnson damping functions, along with the split valence double-ζ def2-SVP basis set.[15–20] Full geometric optimizations performed with this method yielded theoretical structures in good agreement with those determined experimentally from single-crystal X-ray measurements, which has been demonstrated to be a good metric in the assessing the accuracy of a periodic simulation, with a maximum average absolute error of $\approx$3%.[21] Vibrational analyses were then performed using the optimized structures within the harmonic approximation with two-point displacement scheme, affording Γ-point vibrational transition frequencies and normal modes.[22] Because anharmonic effects are pronounced in modes with low-transition frequencies,[7] any mode with a transition frequency less than 20 cm^{-1} was corrected through evaluation of the anharmonic vibrational potential obtained by explicitly determining the energy as a function of normal coordinate displacement, at which point the corrected transition frequency was found using the one-dimensional anharmonic oscillator Schrodinger equation.[7,23] The influence of each vibration on charge transport was then determined using the dimer projection approach, wherein transfer integral fluctuations induced by independent vibrational modes are found from the classical thermal vibrational amplitude and the non-local electron–phonon coupling.[7,24,25] Additional details regarding the simulations are available in the ESI.†

The investigated systems belong to common classes of molecules that facilitate charge transport, including linear acenes DT-Ant and DT-Pen, the former of which exhibits herringbone packing, polycyclic aromatic hydrocarbon (PAH) pyrene DT-P, and quasi-linear thioacene C6-DT-BTBT. Each of these systems exhibit a co-planar orientation of the σ-bonded thiophene-containing side-groups relative to the fused molecular core, with the exception of DT-Pen, which exhibits an orthogonal arrangement of these groups.

Owing to the unique chemical identities and crystalline structures of the investigated materials, each molecular crystal (unsurprisingly) exhibits a distinct set of low-frequency dynamics, which directly influence charge carrier dynamics. To quantify these impacts, the effective modulation of the intermolecular electronic coupling was calculated as transfer integral fluctuations for each vibrational mode below 400 cm^{-1}, which is determined from calculating the derivative of the transfer integral as a function of normal mode displacement (*i.e.*, non-local electron–phonon coupling), while also accounting for the amplitude of vibrational displacement, which is inversely proportional to the calculated transition frequency.[7] Fig. 2 showcases the mode-resolved transfer integral fluctuations that arise from low-frequency vibrations for each material, as well as the specific molecular motions that are particularly detrimental for charge transport. In the case of DT-Ant, which crystallizes in the same herringbone pattern as the well-known BTBT system, the familiar mode-type involving long-axis molecular sliding induces the largest transfer integral fluctuation.[7,8] This motion has been previously demonstrated to be uniquely harmful for charge transport in systems that exhibit herringbone packing, which is desirable for bulk geometry that promotes high-performance 2-D charge transport systems.[4,5,7]

However, for DT-P and C6-DT-BTBT, torsional motions of the σ-bonded thiophene-containing side-groups induce the largest transfer integral fluctuations, while a similar mode in DT-Ant has the second-largest impact, as shown in Fig. 2. Further, these torsional dynamics persist at comparatively high frequencies. For example, in the case of C6-DT-BTBT, while the vibrations predicted with transition frequencies 103.39 cm^{-1} and 39.52 cm^{-1} are similar in mode-type (Fig. 2), the more

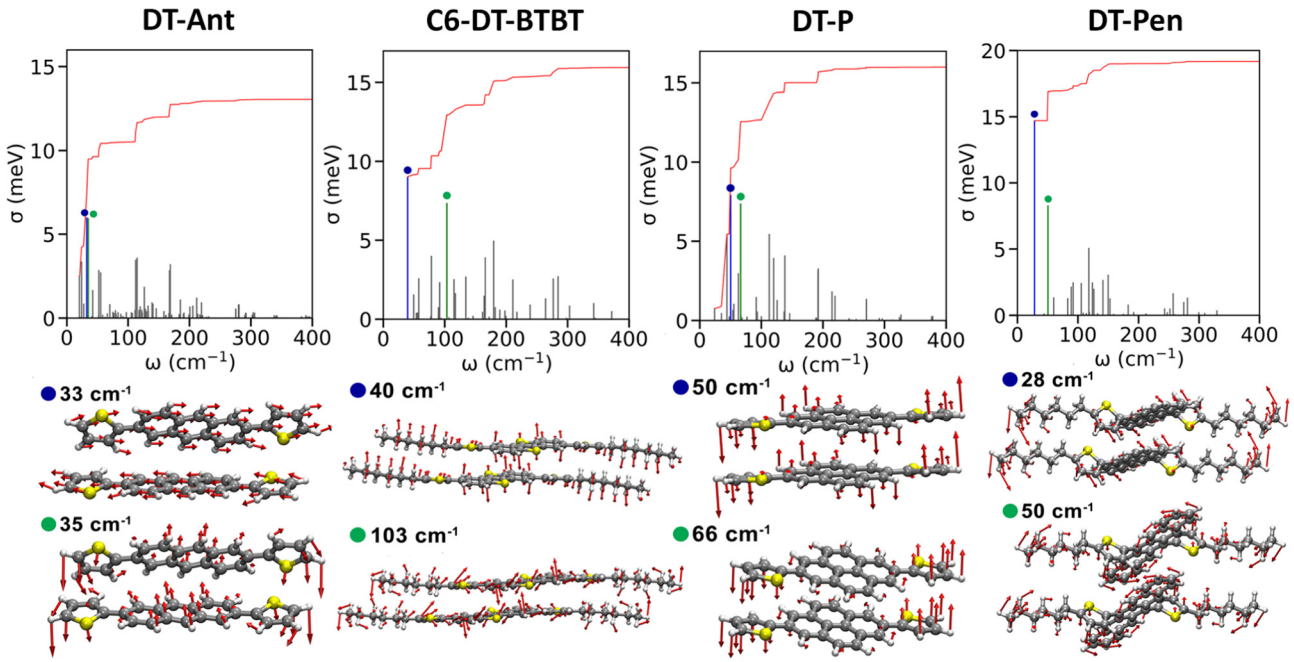

Fig. 2 Transfer integral fluctuations (top) and identified vibrational modes (bottom) for DT-Ant (a), DT-P (b), C6-DT-BTBT (c), and DT-Pen (d), with the cumulative total disorder calculated for each material illustrated with a red line. Modes with large transfer integral fluctuations are noted with green and blue circles on the transfer integral fluctuation figures, with red arrows illustrating atomic displacement. Alkyl chain displacements have been scaled to 30% of the predicted eigenvectors for visual clarity.

pronounced torsional dynamics of the former mode results in a comparatively larger electron–phonon coupling than the latter (18 and 10 meV, respectively, Fig. S3, ESI†). However, the vibration with more modest torsional displacements produces a greater transfer integral fluctuation than the more pronounced mode, due to the larger amplitude of displacement as a result of the lower transition frequency (Fig. 2).

This is not the case for DT-Pen, where the most detrimental vibrations involve hindered-rotational mode-types about the axis normal to the molecular plane, and only slight torsional motions of side-groups. This implies that dynamics of the thiophene groups play a less pivotal role in this system, compared to the other investigated materials. Though the material shares the commonality of σ-bonded thiophene rings, motions of these groups do not meaningfully impede charge transport for this material. However, DT-Pen is unique amongst this family, as it is the only investigated material with a perpendicular orientation of the thiophene groups with respect to the molecular core. Close inspection of the HOMO electronic structure for each material showcases that in the co-planar systems, the aromatic thiophene ring strongly participates in the conjugated π-system. The perpendicular orientation of DT-Pen yields a HOMO electronic structure with only a minor amount of electron density on the σ-bonded thiophene rings, which have significantly larger HOMO expansion coefficients in the aforementioned materials with planar orientations of these groups (Fig. 3).

As a result, it appears that torsional dynamics are particularly detrimental for co-planar orientations of σ-bonded thiophene-containing side-groups. This is because such motions meaningfully

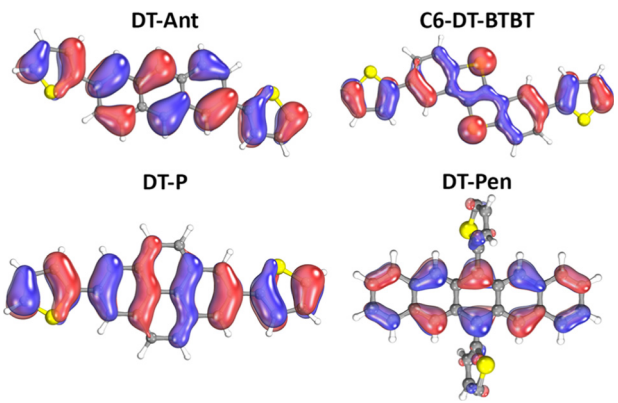

Fig. 3 HOMO electronic structures of the investigated materials. Alkyl chains of C6-DT-BTBT and DT-Pen have been excluded for visual clarity.

disturb the intermolecular overlap of electron density that is strongly delocalized among these rings, which prominently modulates the coupling of molecular wavefunctions. In order to further investigate this hypothesis, the torsional motions of the identified detrimental modes for each material were artificially removed by only displacing atoms in the molecular core along the normal coordinate, while the displacement vectors for the atoms of side-groups were set to zero, locking them into their equilibrium orientation. Re-evaluation of the non-local electron–phonon couplings in this manner significantly reduces the impact of these motions, with direct implications on the magnitude of transfer integral fluctuations and consequent dynamic disorder for DT-Ant, DT-P, and C6-DT-BTBT, with the largest change ($\approx -77\%$) occurring

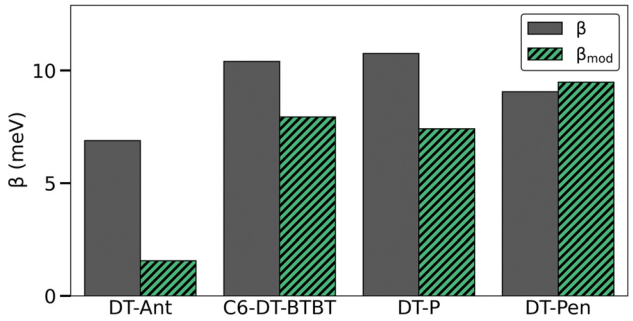

Fig. 4 Calculated non-local electron–phonon coupling values (β) for the identified vibrational modes with torsional motions of side-chains for the investigated materials. The standard term is illustrated in gray, while the term calculated using structures that artificially preserve the equilibrium orientation of the side-groups is illustrated in dashed green.

for DT-Ant. However, in the case of DT-Pen, this re-evaluation only slightly modulates the electron–phonon coupling term ($\approx$+5%), and in fact represents a slightly more detrimental mode-type than the unmodified vibration, as illustrated in Fig. 4. Ultimately, this validates the premise that for systems with perpendicular arrangements of these aromatic side-groups, torsional side-chain motions do not induce significant transfer integral fluctuations, and are less critical for charge transport.

Thus, while the hypothesis that σ-bonded thiophene groups might enhance intermolecular π–π and S–π interactions, the equilibrium conformation and resulting low-frequency dynamics must be strongly considered when designing new materials. It is clearly apparent that a co-planar orientation of the thiophene substituent results in an extension of the aromatic system to the side chain, and when coupled with relatively soft torsional potential, promotes significant displacement of such groups at low frequencies. Because these low-frequency modes are highly-excited at ambient conditions (k_bT_{298} = 207.1 cm^{-1}), such dynamics play an important role in modulating charge carrier dynamics. However, as the thiophene substituent deviates from a co-planar arrangement with the fused core, its participation in the aromatic system diminishes, effectively reducing the impact from associated torsional dynamics on charge transport properties. In this regard, it is important to emphasize that all of the studied materials exhibit torsional motions of their side chains, and it is the equilibrium electronic structure – and how that electronic structure is perturbed by vibrations – that ultimately dictates the impact on electron–phonon coupling.

Overall, this study investigates the low-frequency dynamics of a sample of organic semiconducting materials bearing similar thiophene-containing side groups. In a general case for these materials, torsional dynamics involving these groups were found to strongly influence intermolecular electronic couplings when these side-groups are arranged with planar orientations with respect to the central molecular core, while perpendicular orientations reduce the impact of such dynamics on charge transport. While this communication is focused upon σ-bonded thiophene rings, these results motivate future studies for related substituents. This work emphasizes the underlying connection between molecular conformation, low-frequency vibrational dynamics, and semiconducting performance. Additionally, these results highlight the care that must be taken when designing prospective molecules for organic electronic devices, which must consider low-frequency vibrational dynamics and their implications for intermolecular electronic couplings.

M. T. R. and P. A. B. thank the National Science Foundation (DMR-2046483) for financial support.

Conflicts of interest

There are no conflicts to declare.

Notes and references

1 H. Sirringhaus, *Adv. Mater.*, 2014, **26**, 1319–1335.
2 S. Ciuchi and S. Fratini, *Phys. Rev. B: Condens. Matter Mater. Phys.*, 2012, **86**, 245201.
3 V. Coropceanu, J. Cornil, D. A. da Silva Filho, Y. Olivier, R. Silbey and J. L. Brédas, *Chem. Rev.*, 2007, **107**, 926–952.
4 S. Fratini, M. Nikolka, A. Salleo, G. Schweicher and H. Sirringhaus, *Nat. Mater.*, 2020, **19**, 491–502.
5 T. Okamoto, C. P. Yu, C. Mitsui, M. Yamagishi, H. Ishii and J. Takeya, *J. Am. Chem. Soc.*, 2020, **142**, 9083–9096.
6 A. Yamamoto, Y. Murata, C. Mitsui, H. Ishii, M. Yamagishi, M. Yano, H. Sato, A. Yamano, J. Takeya and T. Okamoto, *Adv. Sci.*, 2018, **5**, 1700317.
7 G. Schweicher, G. D'Avino, M. T. Ruggiero, D. J. Harkin, K. Broch, D. Venkateshvaran, G. Liu, A. Richard, C. Ruzie, J. Armstrong, A. R. Kennedy, K. Shankland, K. Takimiya, Y. H. Geerts, J. A. Zeitler, S. Fratini and H. Sirringhaus, *Adv. Mater.*, 2019, **31**, 1902407.
8 S. Illig, A. S. Eggeman, A. Troisi, L. Jiang, C. Warwick, M. Nikolka, G. Schweicher, S. G. Yeates, Y. Henri Geerts, J. E. Anthony and H. Sirringhaus, *Nat. Commun.*, 2016, **7**, 1–10.
9 H. Chung, D. Dudenko, F. Zhang, G. D'Avino, C. Ruzié, A. Richard, G. Schweicher, J. Cornil, D. Beljonne, Y. Geerts and Y. Diao, *Nat. Commun.*, 2018, **9**, 1–12.
10 K. Takimiya, S. Shinamura, I. Osaka and E. Miyazaki, *Adv. Mater.*, 2011, **23**, 4347–4370.
11 Y. Qiao, J. Zhang, W. Xu and D. Zhu, *Tetrahedron*, 2011, **67**, 3395–3405.
12 H. Meng, F. Sun, M. B. Goldfinger, G. D. Jaycox, Z. Li, W. J. Marshall and G. S. Blackman, *J. Am. Chem. Soc.*, 2005, **127**, 2406–2407.
13 J. Wang, K. Liu, Y. Y. Liu, C. L. Song, Z. F. Shi, J. B. Peng, H. L. Zhang and X. P. Cao, *Org. Lett.*, 2009, **11**, 2563–2566.
14 N. Miyaura, T. Ishiyama, M. Ishikawa and A. Suzuki, *Tetrahedron Lett.*, 1986, **27**, 6369–6372.
15 R. Dovesi, A. Erba, R. Orlando, C. M. Zicovich-Wilson, B. Civalleri, L. Maschio, M. Rérat, S. Casassa, J. Baima, S. Salustro and B. Kirtman, *Wiley Interdiscip. Rev.: Comput. Mol. Sci.*, 2018, **8**, e1360.
16 R. Dovesi, A. Erba, R. Orlando, C. M. Zicovich-Wilson, B. Civalleri, L. Maschio, M. Rérat, S. Casassa, J. Baima, S. Salustro and B. Kirtman, *Wiley Interdiscip. Rev.: Comput. Mol. Sci.*, 2018, **8**, e1360.
17 J. P. Perdew, K. Burke and M. Ernzerhof, *Phys. Rev. Lett.*, 1996, **77**, 3865–3868.
18 S. Grimme, *Wiley Interdiscip. Rev.: Comput. Mol. Sci.*, 2011, **1**, 211–228.
19 S. Grimme, S. Ehrlich and L. Goerigk, *J. Comput. Chem.*, 2011, **32**, 1456–1465.
20 F. Weigend and R. Ahlrichs, *Phys. Chem. Chem. Phys.*, 2005, **7**, 3297–3305.
21 P. A. Banks, Z. Song and M. T. Ruggiero, *J. Infrared, Millimeter, Terahertz Waves*, 2020, **41**, 1411–1429.
22 F. Pascale, C. M. Zicovich-Wilson, F. López Gejo, B. Civalleri, R. Orlando and R. Dovesi, *J. Comput. Chem.*, 2004, **25**, 888–897.
23 M. Hutereau, P. A. Banks, B. Slater, J. A. Zeitler, A. D. Bond and M. T. Ruggiero, *Phys. Rev. Lett.*, 2020, **125**, 103001.
24 B. Baumeier, J. Kirkpatrick and D. Andrienko, *Phys. Chem. Chem. Phys.*, 2010, **12**, 11103–11113.
25 E. F. Valeev, V. Coropceanu, D. A. Da Silva Filho, S. Salman and J. L. Brédas, *J. Am. Chem. Soc.*, 2006, **128**, 9882–9886.

